Coupled harmonic oscillators for the measurement of a weak classical force at the standard quantum limit

Paola Leaci[1,*] and Antonello Ortolan[2]
[1]*Department of Physics, University of Trento and INFN Trento, I-38100 Povo, Trento, Italy*
[2]*INFN Laboratori Nazionali di Legnaro, I-35020 Legnaro, Padova, Italy*
(Received 13 June 2007; published 4 December 2007)

We discuss limitations in precision measurements of a weak classical force coupled to quantum mechanical systems, the so-called standard quantum limit (SQL). Among the several contexts exploiting the measurement of classical signals, gravitational wave (GW) detection is of paramount importance. In this framework, we analyze the quantum limited sensitivity of a free test mass, a quantum mechanical harmonic oscillator, two harmonic oscillators with equal masses and different resonance frequencies, and finally two mechanical oscillators with different masses and resonating at the same frequency. The sensitivity analysis of the latter two cases illustrates the potentialities of back-action reduction and classical impedance matching schemes, respectively. By examining coupled quantum oscillators as detectors of classical signals, we found a viable path to approach the SQL for planned or operating GW detectors, such as DUAL and AURIGA.

DOI: 10.1103/PhysRevA.76.062101 PACS number(s): 03.65.Ta, 95.55.Ym, 04.80.Nn, 42.50.Dv

I. INTRODUCTION

The standard quantum limit (SQL), defined more than 30 years ago [1], represents the sensitivity limit for a linear position meter (sometimes called *coordinate meter*) imposed by quantum mechanics. The device monitors the position $x(t)$ of a free test mass, and thereby deduces the classical force signal $F_s(t)$ that acts on a mass.

In principle a macroscopic mass will exhibit quantum behavior if, first, its displacement can be measured with sufficient accuracy and, second, thermal, seismic, and electronic readout noises can be adequately reduced. In this case the momentum and displacement uncertainties are given by the Heisenberg uncertainty principle, which imposes fundamental [35] restrictions on the accuracy of macroscopic measurements.

In the 1970s, in connection with efforts to operate gravitational wave (GW) detectors, it became crucial to envisage methods for measuring macroscopic observables at levels of precision approaching and/or exceeding the SQL. This represents the first goal for the measuring sensitivity of an apparatus devised to detect a weak classical force. A typical example is the interferometric position measurement, where the monitored free test mass is generally one of the mirrors of the interferometer [1,2]. On the other hand, the applications of quantum oscillators coupled to classical signals are relevant in many high-precision experiments, i.e., general relativity tests, in gravimeters, accelerometers, gyroscopic devices, etc. [3]. In particular, free masses (interferometers) or mechanical oscillators (resonant bars) are employed as GW detectors.

In Ref. [1], the authors formulated the concept of SQL for high-precision measurements and demonstrated also that the SQL can be overcome by changing the instrument designs. Nowadays, approaching or beating the SQL is one of the most attractive experimental challenges [4]: of the many proposed approaches, we must mention techniques to eliminate the back-action contribution in quantum measurements [5,6], methods for quantum nondemolition measurements [3,7–9], and the use of speed meters [10]. However, the most promising approaches seem to be innovative nanotechnologies, where very small mechanical oscillators are coupled to high-sensitivity electronics [11,12] and advanced GW interferometers [13].

In this paper we present the quantum noise analysis of a system of two coupled oscillators. Our analysis makes it clear that, for an experimental detection of weak forces, a system of two oscillators is more suitable than a single oscillator as its noise stiffness can be more easily adapted to a quantum limited amplifier. In particular, we compare the performances of a system of two harmonic oscillators with equal masses and different resonance frequencies (weak coupling), and with different masses and resonating at the same frequency (tight coupling). The two cases are of some relevance as they illustrate the potentialities of back-action reduction and classical impedance matching schemes for measurements of a weak force. As concrete examples of the two schemes, we analyze in some detail the planned DUAL detector [14] and the operating AURIGA resonant detector [15], respectively.

The paper is organized as follows. In Sec. II we discuss in detail the quantum limits in the detection of a classical force coupled to free or interacting particles. In Sec. III we apply the SQL formalism to a system of two equal mass harmonic oscillators with different resonance frequencies and to a couple of harmonic oscillators with different masses and the same resonance frequency. For the latter system, the thermal noise effect has been also calculated. Conclusions are drawn in Sec. IV.

II. QUANTUM LIMITS FOR THE DETECTION OF A CLASSICAL FORCE

As is well-known, the uncertainty principle states that one cannot assign exact simultaneous values to the position and

*Corresponding author. leaci@science.unitn.it

momentum of a quantum mechanical system. Rather, we can only determine such quantities with some characteristic "uncertainties," Δx and Δp, which satisfy the inequality

$$\Delta x \Delta p \geq \frac{\hbar}{2}, \tag{1}$$

where $\Delta x = [\int_{-\infty}^{+\infty} \mathcal{P}(x)(x-\bar{x})^2 dx]^{1/2}$ and $\Delta p = [\int_{-\infty}^{+\infty} \Pi(p)(p-\bar{p})^2 dp]^{1/2}$ are the standard deviations of x and p, respectively, $\bar{x}$ and $\bar{p}$ their mean values, and $\mathcal{P}$ and Π their probability density functions, given by the modulus squared of solutions of the Schrödinger equation with suitable boundary conditions. The variances of these two random variables are related to their power spectral densities by $(\Delta x)^2 = \int_{-\infty}^{+\infty} S_x(\omega) d\omega$ and $(\Delta p)^2 = \int_{-\infty}^{+\infty} S_p(\omega) d\omega$, where S_x (m^2/Hz) is the displacement noise power spectral density contributed by the readout, and S_p (N^2/Hz^3) is the impulse spectral density.

The SQL is a probe characteristic and can be evaluated by using a quantum measuring device that operates under the intrinsic noise condition $S_x S_F = \hbar^2/4$ [1], where the spectral density of the fluctuating back-action force, $S_F(\omega)$ (N^2/Hz), is equal to $S_p(\omega)$ multiplied by ω^2.

By optimization of a measurement device at a particular frequency, we mean that the device works at the SQL at that frequency. A nonoptimized measuring device would spoil the SQL sensitivity. In order to build an optimized measuring apparatus, we have to specify the probe and how the measuring device acts on the probe. When one measures a classical force by the induced motion on a probe (e.g., a free mass or an oscillator), different SQLs can be defined, depending on the dynamics of the system. For example, the well-known case of SQL of a free mass depends on the time interval between the two successive position measurements, whereas the SQL of an oscillator also depends on its resonant frequency [1,3]. In general, we can replace the inequality in Eq. (1) with

$$S_x S_F \geq \frac{\hbar^2}{4}, \tag{2}$$

which establishes a universal, mutual connection between the accuracy of the monitoring and the perturbation of the monitored object [1].

To compute the minimum detectable amplitude $F_{\min}$ of a probe at unitary signal-to-noise ratio (SNR), we define the standard force signal $F_s(t)$ as a sinusoid at frequency ω_F that lasts for the time interval $\left[-\frac{\tau_F}{2}, +\frac{\tau_F}{2}\right]$. The Fourier transform of $F_s(t)$ reads

$$F_s(\omega) = \tau_F F_0 \,\mathrm{sinc}\left[\frac{\tau_F}{2}(\omega + \omega_F)\right], \tag{3}$$

where F_0 is the force amplitude. For optimal signal processing, the maximum achievable SNR is given by [16]

$$\mathrm{SNR} = \frac{1}{2\pi}\int_{-\infty}^{+\infty} \frac{|F_s(\omega)|^2}{S(\omega)} d\omega, \tag{4}$$

where $S(\omega)$ is the total force noise at the detector output. By solving Eq. (4) with SNR=1 we have $F_{\min} = \left\{\frac{1}{2\pi}\int_{-\infty}^{+\infty} \mathrm{sinc}^2\left[\frac{\tau_F}{2}(\omega+\omega_F)\right]/S(\omega) d\omega\right\}^{-1/2}/\tau_F$. In the limit of $\tau_F \to 0$, the classical impulsive force signal can be represented by $F = P_0 \delta(t)$, where P_0 is the total exchanged momentum. In this case, the minimum detectable impulse at SNR=1 can be easily calculated as $P_{\min} = \lim_{\tau_F \to 0} \tau_F F_{\min}$.

GWs are an example of a weak classical perturbation, where the response of the measuring device probe-object may be comparable to its quantum mechanical uncertainties. Moreover, the weakness of the interaction ensures that no back-action of the probe affects the GW radiation field. Consequently, the gravitational signal acts on the probe as a "classical force" (i.e., a force that is independent of the probe quantum state) [1]. From the theory of general relativity follows the expression of the classical force for a GW impinging on a detector [17],

$$F(t) = \frac{1}{2} M_{eff} L_{eff} \ddot{h}(t), \tag{5}$$

where M_{eff} and L_{eff} are the effective mass and length of the GW detector.

The sensitivity of all GW detectors is limited by the SQL, which disallows repeated measurements of the relevant observables with arbitrary precision. Of course, a GW detector can reach the SQL performances only if it employs a quantum limited readout system. For instance, the capacitive readout developed at the University of Trento is based on superconducting quantum interference device (SQUID) amplifiers [18]: the best energy resolution achieved is a few $\hbar$ [19] and the single-quantum sensitivity appears within reach.

From Eq. (5), the sensitivity of GW detectors is given as the noise power spectral density in terms of the wave amplitude referred to at the input,

$$S_{hh}(\omega) = \left(\frac{2}{M_{eff} L_{eff} \omega^2}\right)^2 S(\omega) \quad 1/\mathrm{Hz}. \tag{6}$$

For GW burst signals, a useful relation is their minimum amplitude, obtained with unity SNR, $h_{\min} \approx (2F_{\min})/(M_{eff} L_{eff} \omega_p^2)$, where ω_p is the probe angular frequency. For other signals (e.g., stochastic background, periodic signals or, loosely speaking, signals with strong frequency structures in the detector band), the appropriate sensitivity indicator is the minimum of the corresponding noise spectral density, $S_{hh}^{\min}$, and the bandwidth. However, if the ratio between the detector band, $\Delta\omega$, and ω_p is <1, we have [20]

$$S_{hh}^{\min} \approx \frac{(2h_{\min})^2}{\omega_p^2} \Delta\omega, \quad \Delta\omega \approx \frac{k_n}{M_{eff}\omega_p}, \tag{7}$$

where the parameter $k_n = (S_F/S_x)^{1/2}$ represents the readout noise stiffness required to optimize the performances of the detector, by achieving the best impedance matching with the readout system [21]. The force and displacement noises can be parametrized as $S_F \equiv n\hbar k_n$ and $S_x \equiv n\hbar/k_n$, respectively, where n is the energy resolution of the probe expressed as the number of quanta at the amplifier frequency, and the SQL is recovered in the limit $n \to 1/2$.

III. GW DETECTORS AT SQL

We want to discuss the minimum detectable amplitude of a classical force acting on a free particle, an oscillator, and a system of two coupled oscillators at their respective SQLs. The sensitivity limits of a free test mass and a single harmonic oscillator have been already studied [1]; here we only report the main results preparatory to the sensitivity computation of two coupled harmonic oscillators with equal masses and different resonance frequencies (weak coupling), and of two mechanical oscillators with different masses and resonating at the same frequency (tight coupling).

In what follows we will consider linear position meters (amplifiers), with the position and force noises uncorrelated and the corresponding spectral densities, S_x and S_F, and their ratio k_n^2 frequency independent [16]. These spectral densities, which the meter exerts on the test mass, must satisfy the uncertainty relation expressed by Eq. (2). On the other hand, to get the SQL sensitivity, two requirements have to be satisfied: (i) the noise sources have to be as small as possible [i.e., the equality in Eq. (2) holds]; and (ii) the total force noise has to reach its minimum (i.e., the noise stiffness matches the amplifier at a given frequency ν_a).

It is worth noticing that the SQL sensitivity curve can be considered as an envelope of the minimum of many sensitivity curves, corresponding to different amplifiers matched to different k_n. However, in practice, the same amplifier can be optimized over a frequency band, where its sensitivity curve overlaps closely the SQL curve, and so k_n can be considered independent of frequency within this band.

The total noise in a measurement at the SQL can be described by its (bilateral) spectral density $S(\omega)$, which we will specialize to some relevant systems for the GW detection, namely, a free particle (interferometric detector), an oscillator (single mode resonant detector), and a system of two coupled oscillators: weak coupling for the back-action reduction and high coupling for the impedance matching.

A. Free test mass

The equation of motion referring to the linear detection scheme of an external classical force, $F_{fm}(t)$, acting on the free test mass, m, is equal to

$$F_{fm}(t) - F_{fl}(t) - m\frac{d^2}{dt^2}x_{fl}(t) = 0, \tag{8}$$

where $x_{fl}(t)$ is the additive noise of the meter and $F_{fl}(t)$ is its back-action force noise.

From Eq. (8), the spectral density of the total noise readily follows:

$$S_{fm}(\omega) = m^2\omega^4 S_x + S_F. \tag{9}$$

For any given amplifier optimization frequency $\omega_a = 2\pi\nu_a$, $S_{fm}(\omega)$ can be minimized by adjusting the ratio of the spectral densities $S_F/S_x = m^2\omega_a^4$, and the corresponding SQL power spectral density is $S_{fm}^{\mathrm{SQL}}(\omega_a) = \hbar m\omega_a^2$ [16]. In effect, the sensitivity of a measuring device can be largely optimized by adjusting the S_F/S_x ratio.

The total force noise power spectral density, obtained by optimizing the amplifier at ω_a, is

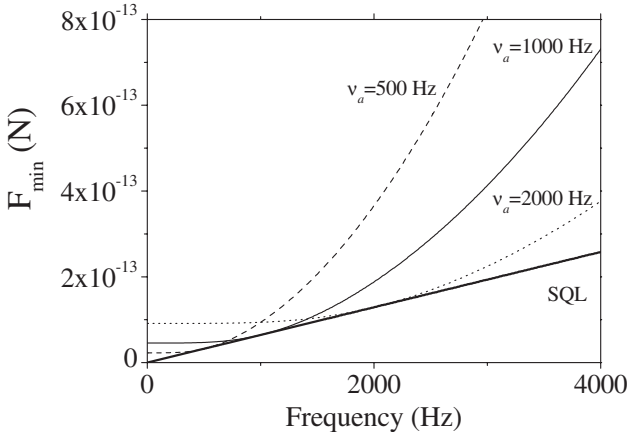

FIG. 1. Comparison between the minimum detectable amplitude of a force acting on a free particle, at different values of the frequency $\nu_a = \omega_a/(2\pi)$, and at the SQL; $m = 1$ kg and $\tau_F = 1$ s.

$$S_{fm}(\omega) = \frac{\hbar m}{2}\left(\frac{\omega^4}{\omega_a^2} + \omega_a^2\right), \tag{10}$$

where $S_{fm}(\omega) \to S_{fm}^{\mathrm{SQL}}(\omega)$ for $\omega \to \omega_a$.

Figure 1 shows the minimum detectable amplitude of an impulsive force lasting for a time $\tau_F = 1$ s, acting on the free test mass at the SQL (bold solid line), $F_{fm}^{\mathrm{SQL}}(\omega) = \sqrt{\frac{\hbar m}{\tau_F}}\omega$, and the force obtained by optimizing the amplifier at ω_a:

$$F_{fm}(\omega) = \sqrt{\frac{\hbar m}{\tau_F}}\omega\left[\frac{1}{2}\left(\frac{\omega^2}{\omega_a^2} + \frac{\omega_a^2}{\omega^2}\right)\right]^{1/2}. \tag{11}$$

Each curve in Fig. 1 is tangent to the SQL curve just at the frequency where, from time to time, we have optimized k_n^2.

B. Harmonic oscillator

In the case of an oscillator of mass m_o and angular resonant frequency ω_o, the equation of motion is

$$F_o(t) - F_{fl}(t) - m_o\left(\frac{d^2}{dt^2} + \omega_o^2\right)x_{fl}(t) = 0, \tag{12}$$

where $F_o(t)$ is the external force acting on the oscillator. In the frequency domain, and in the presence of dissipative forces, the equation of motion is

$$F_o(\omega) - F_{fl}(\omega) + m_o\omega^2 x_{fl}(\omega) - m_o\omega_o^2\left[1 + \frac{i}{Q}\right]x_{fl}(\omega) = 0, \tag{13}$$

where Q is the quality factor of a low loss material and $m_o\omega_o^2[1 + i/Q]$ the complex spring constant. Here we assume the losses are independent of frequency and the relation $\phi = 1/Q$ holds, where ϕ is the phase lag [22]. The power spectral density associated with $F_o(\omega)$ in Eq. (13) is

$$S_o(\omega) = m_o^2\left[(\omega_o^2 - \omega^2)^2 + \frac{\omega_o^4}{Q^2}\right]S_x + S_F. \tag{14}$$

The spectral densities S_x and S_F satisfy Eq. (2) in the SQL conditions. By adjusting k_n^2, we can provide the minimum of

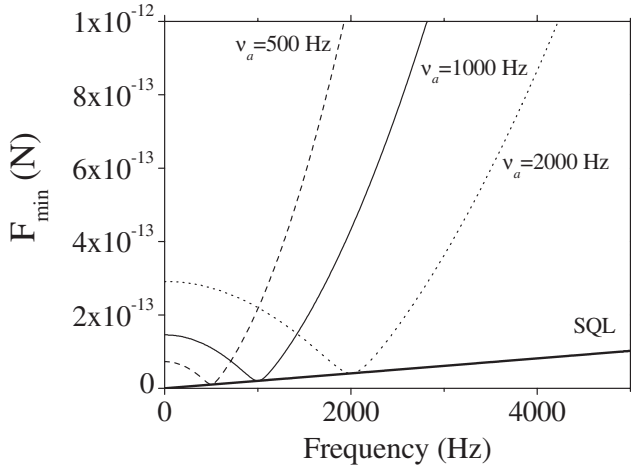

FIG. 2. Comparison between the minimum detectable amplitude of a force acting on an oscillator, for different values of $\nu_a = \omega_a/(2\pi)$, and at the SQL; $m_o=1$ kg, $Q=10$, and $\tau_F=1$ s.

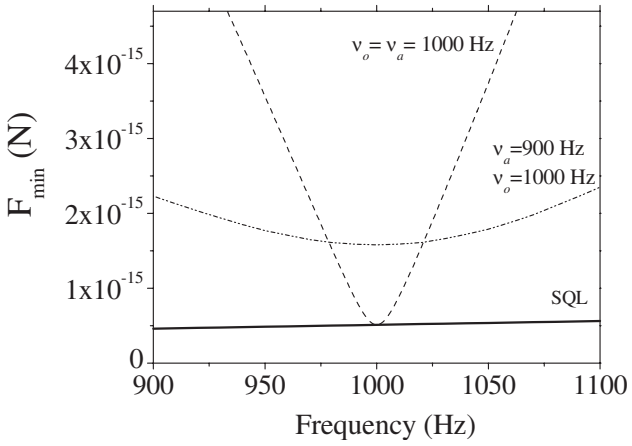

FIG. 3. Comparison of the minimum detectable amplitudes of a force acting on the oscillator, at the SQL (bold solid line), and with the amplifier optimized at frequency ν_a: (i) $\nu_a=\nu_o$ (dashed line) and (ii) $\nu_a \neq \nu_o$ (dashed-dotted line); $m_o=1$ kg, $Q=10^2$, and $\tau_F=10^3$ s; $\nu_o=\omega_o/(2\pi)$.

spectral density in some interesting physical situations (as shown in Fig. 2).

(i) The bold solid line corresponds to the minimum detectable amplitude for a force that lasts for a time $\tau_F=1$ s and acts on the oscillator at the SQL,

$$F_o^{\mathrm{SQL}}(\omega) = \sqrt{\frac{\hbar m_o}{Q\tau_F}}\omega. \tag{15}$$

(ii) The thin curves represent the amplitude obtained by optimizing the amplifier at specific oscillator resonant frequencies ($\nu_o=\nu_a$),

$$F_{o;\omega_a} = \sqrt{\frac{\hbar m_o}{Q\tau_F}}\omega\left\{\frac{1}{2}\left[(Q^2+2)\frac{\omega_o^2}{\omega^2} + \left(\frac{\omega^2}{\omega_o^2}-2\right)Q^2\right]\right\}^{1/2}. \tag{16}$$

In Fig. 3 we show the minimum amplitude of the force calculated by optimizing the amplifier at a frequency ν_a, equal (dashed line) and different (dashed-dotted line) from ν_o,

$$F_{o;\omega_a} = \sqrt{\frac{\hbar m_o}{\tau_F}}\left\{\frac{(\omega^2-\omega_o^2)^2 + (\omega_a^2-\omega_o^2)^2 + 2\omega_o^4/Q^2}{2[(\omega_o^2-\omega_a^2)^2 + \omega_o^4/Q^2]^{1/2}}\right\}^{1/2}, \tag{17}$$

and the SQL curve defined as in Fig. 2.

Notice that the above expression reduces to Eq. (16) for $\omega_a=\omega_o$. In fact, the width of the minimum depends on $\omega_a^2 - \omega_o^2$ as long as $|\omega_a-\omega_o| > (\omega_a+\omega_o)/(2Q)$, as shown in Fig. 3. In addition, the distance between the dashed-dotted and the bold solid (SQL) lines depends on the Q value, and the two curves will lie close together as Q increases. Equations (15)–(17) were calculated by imposing SNR=1 in Eq. (4), with the integrand function depending on the frequency we choose to optimize. The spectral noise densities we substituted in Eq. (4) to calculate Eqs. (15)–(17) are given by

$$S_o^{\mathrm{SQL}}(\omega) = \hbar m_o\left[(\omega_o^2-\omega^2)^2 + \frac{\omega_o^4}{Q^2}\right]^{1/2}, \tag{18}$$

$$S_o(\omega) = \hbar m_o\left\{\left[(\omega_o^2-\omega^2)^2 + \frac{\omega_o^4}{Q^2}\right]\frac{Q}{2\omega_o^2} + \frac{\omega_o^2}{2Q}\right\}, \tag{19}$$

and

$$S_o(\omega) = \frac{\hbar m_o}{2\sqrt{(\omega_o^2-\omega_a^2)^2 + \frac{\omega_o^4}{Q^2}}}\left\{\left[(\omega_o^2-\omega^2)^2 + \frac{\omega_o^4}{Q^2}\right] + \left[(\omega_o^2-\omega_a^2)^2 + \frac{\omega_o^4}{Q^2}\right]\right\}, \tag{20}$$

respectively. It is worth noticing that to obtain Eq. (15), we considered in Eq. (4) the square of $F_s(\omega)$ with $\omega_F=\omega_0$, while in order to find Eqs. (16) and (17) we used just the square of $F_s(\omega)$. Also for an interacting particle, the intersection between each curve of Fig. 2 with the SQL curve occurs at the frequency where, from time to time, we have optimized k_n^2.

The advantage to consider an oscillator is evident from Fig. 4, where we compare its behavior with that of a free mass. In particular, the SQL of minimum detectable amplitude for a force acting on an oscillator lies below the corresponding limit for a free test mass. This is due to the Q factor that, for temperatures approaching absolute zero, is a dimensionless measure of dissipation at the oscillator resonant frequency [22]. Moreover, from the dotted line in Fig. 4, we note a narrowing of the bandwidth, with a minimum force amplitude in correspondence with the oscillator resonant frequency.

C. Coupled harmonic oscillators

In the field of GW detection, detector designs usually involve two or more coupled harmonic oscillators. The im-

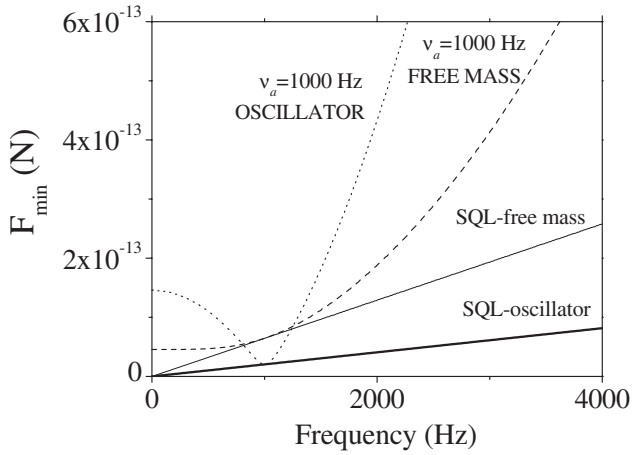

FIG. 4. Minimum amplitude force acting on a free and interacting test mass. In this case, $m_o=m=1$ kg, $Q=10$, and $\tau_F=1$ s.

provements of the detector sensitivity arise either from impedance matching or back-action reduction [21]. Up to now, resonant transducers have been widely adopted for resonant detectors to match the mechanical impedance to the SQUID amplifier (see e.g., Ref. [23]); however, the advanced wideband acoustic DUAL detector exploits a novel back-action reduction scheme [14].

1. Weak coupling with different resonant frequencies

Let us consider two weakly coupled quantum mechanical harmonic oscillators, each having the same mass and mechanically resonating at different frequencies. This is the suitable model for a wideband acoustic GW DUAL detector [14], which consists of two concentric massive bodies, two cylinders or two spheres.

The model of the DUAL detector that we consider in this paper is sketched in Fig. 5; it consists of a simple one-dimensional system, with two mechanical harmonic oscillators. This is a crude approximation of a DUAL system; indeed for a three-dimensional body, the dynamics of elastic deformations is given as the superposition of the dynamics of a huge number of normal modes of vibration (for a detailed discussion see Refs. [14,24]). However, the model of two oscillators weakly coupled is accurate enough to study the SQL sensitivity of a DUAL detector.

The equations for the two resonators read

$$F_D(t) - F_{ba}(t) - m_1 \frac{d^2}{dt^2} x_1(t) - k_{n_1}\left[1 + \frac{i}{Q_1}\right] x_1(t) = 0,$$

$$F_D(t) + F_{ba}(t) - m_2 \frac{d^2}{dt^2} x_2(t) - k_{n_2}\left[1 + \frac{i}{Q_2}\right] x_2(t) = 0, \tag{21}$$

where $F_{ba}(t)$ is the back-action force and $F_D(t)$ is the external force acting on two different mechanical resonators, evaluated by a differential measurement of their positions $x_1(t)$ and $x_2(t)$. Here the resonant angular frequencies and the material quality factors for the two resonators are $\omega_{1,2}=(k_{n_{1,2}}/m_{1,2})^{1/2}$ and $Q_{1,2}$, respectively. We measure the differential displacement with an amplifier that is characterized by its additive noise and back-action noise, trying to reach the best coupling between the two resonators and the amplifier [21].

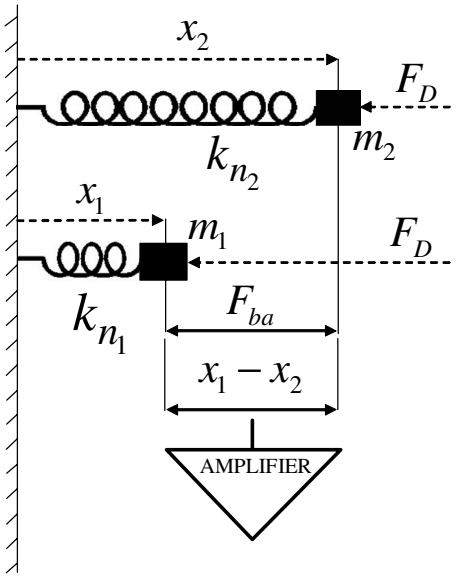

FIG. 5. One-dimensional scheme of a DUAL detector: the force F_D acting on both masses, m_1 and m_2, is measured by the relative displacement, x_1-x_2, of the two oscillators; $k_{n_{1,2}}x_{1,2}$ and F_{ba} are the elastic and back-action forces, respectively.

In fact, by solving Eqs. (21), we obtain in the frequency domain the equation

$$x_d(\omega) = H_{F_D}(\omega)F_D(\omega) - H_{F_{ba}}(\omega)F_{ba}(\omega), \tag{22}$$

where $x_d(\omega)=x_1(\omega)-x_2(\omega)$ is the relative displacement of the two oscillators. The transfer functions of the two resonators are

$$H_{1,2}(\omega) = \frac{1}{-m_{1,2}\omega^2 + m_{1,2}\omega_{1,2}^2\left(1 + \frac{i}{Q_{1,2}}\right)}, \tag{23}$$

represented by solid and dashed lines in Fig. 6, respectively. The transfer functions associated with $F_D(\omega)$ and $F_{ba}(\omega)$ are $H_{F_D}(\omega)=H_1(\omega)-H_2(\omega)$ and $H_{F_{ba}}(\omega)=H_1(\omega)+H_2(\omega)$ (bold solid and dotted lines in Fig. 6, respectively).

The noise power spectral density for the measurement of $F_D(\omega)$, due to the amplifier system, is

$$S_D(\omega) = \frac{S_x + |H_{F_{ba}}(\omega)|^2 S_F}{|H_{F_D}(\omega)|^2}, \tag{24}$$

where the numerator represents the total displacement noise. As in the other cases, by applying the SQL condition, $S_xS_F=\hbar^2/4$, and adjusting the ratio S_F/S_x properly, we obtain the minimum of the considered power spectral density. Then, we can write Eq. (24) as a function of S_x:

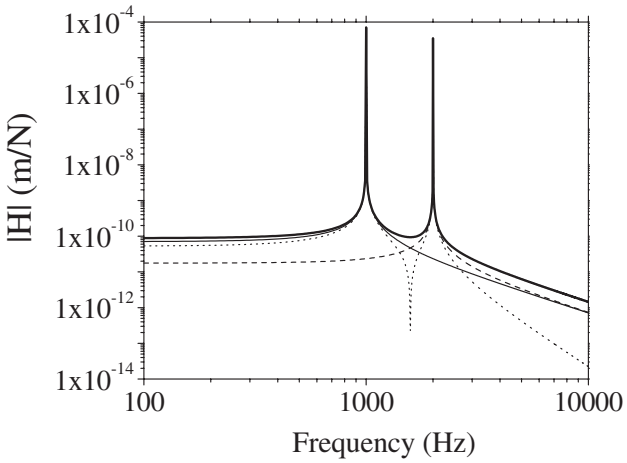

FIG. 6. The solid and dashed lines represent the modulus of the transfer functions of the slow and fast oscillators which correspond, in the three-dimensional case, to the outer and the inner cylinders, respectively. We used $m_1=m_2=10^3$ kg, $Q_1=10^6$, $Q_2=2\times10^6$, $\nu_1=1$ kHz, and $\nu_2=2$ kHz; $\nu_{1,2}=\omega_{1,2}/(2\pi)$. The modulus of the transfer functions $H_{F_D}=H_1-H_2$ (bold solid line) and $H_{F_{ba}}=H_1+H_2$ (dotted line) are also shown. The minimum of this last curve ($\sim$1.6 kHz) is the point of the reduction of the back-action (for a detailed discussion about this topic see Refs. [14,25]).

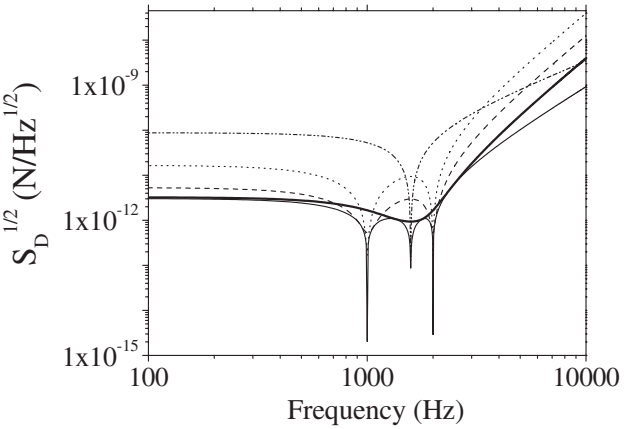

FIG. 7. Optimized noise curves for a DUAL detector. In particular, the solid line represents the noise optimized at every frequency. The other curves refer to different values of S_x in Eq. (25): (i) $S_x=10^{-42}$ m^2/Hz for the dotted curve; (ii) $S_x=10^{-44}$ m^2/Hz for the dashed curve; (iii) $S_x=10^{-45}$ m^2/Hz for the bold solid curve, and (iv) $S_x=10^{-48}$ m^2/Hz for the dashed-dot-dot curve. DUAL parameters as in Fig. 6.

$$S_D(\omega)=\frac{S_x+|H_{F_{ba}}(\omega)|^2\dfrac{\hbar^2}{4S_x}}{|H_{F_D}(\omega)|^2}. \tag{25}$$

Minimizing this equation with respect to S_x, we have

$$S_D(\omega_{\min})=\hbar\frac{|H_{F_{ba}}(\omega_{\min})|}{|H_{F_D}(\omega_{\min})|^2}, \tag{26}$$

which is the lowest noise at $\omega_{\min}$, obtained when the noise power spectral density of the amplifier is $S_x^{\min}=\frac{\hbar}{2}|H_{F_{ba}}(\omega_{\min})|$. The SQL solid curve in Fig. 7, calculated from Eq. (26), shows three minima: two around 1 and 2 kHz, which correspond to the two cylinders' resonance frequencies and one around 1.6 kHz, which represents the back-action reduction. The other curves in Fig. 7 are obtained by replacing different S_x values in Eq. (25): $S_x=10^{-42}$ m^2/Hz for the dotted curve; $S_x=10^{-44}$ m^2/Hz for the dashed curve; $S_x=10^{-45}$ m^2/Hz for the bold solid curve; and $S_x=10^{-48}$ m^2/Hz for the dashed-dot-dot curve. We can see that the curve with a good sensitivity in a wide frequency band is the maximally flat bold solid curve, indicating an optimal coupling between the two oscillators and the amplifier, through a back-action reduction measurement [21].

2. High coupling with equal resonant frequencies

Let us discuss now the problem of two quantum mechanical harmonic oscillators, strongly coupled, with different masses and the same resonance frequency. This is the typical configuration of resonant GW detectors, where the two oscillators represent the bar fundamental mode coupled with the resonant (capacitive [26] or inductive [27]) transducer. As an example of two highly coupled oscillators, we can consider the AURIGA detector [28], designed to measure the force signal due to GWs acting on an aluminum cylinder (the bar), in a frequency band around its fundamental normal mode ($\sim$900 Hz). The equations of motion of the two oscillators, which represent bar and transducer, in the frequency domain read [26]

$$\mathcal{B}(\omega)\begin{pmatrix}x(\omega)\\ y(\omega)\end{pmatrix}-\begin{pmatrix}F(\omega)+F_{ba}(\omega)\\ -F_{ba}(\omega)\end{pmatrix}=0,$$

where $x(\omega)$ and $y(\omega)$ are the displacements of the bar and the transducer and

$$\mathcal{B}(\omega)=M_b\begin{pmatrix}-\omega^2+\omega_b^2\left(1+\dfrac{i}{Q_b}\right)+\mu\omega_{tr}^2\left(1+\dfrac{i}{Q_{tr}}\right) & -\mu\omega_{tr}^2\left(1+\dfrac{i}{Q_{tr}}\right)\\ -\mu\omega_{tr}^2\left(1+\dfrac{i}{Q_{tr}}\right) & \mu\left[\omega_{tr}^2\left(1+\dfrac{i}{Q_{tr}}\right)-\omega^2\right]\end{pmatrix};$$

TABLE I. Masses, resonant frequencies, and Q factors of the AURIGA detector together with the bar length, L_b, and the optimization frequency of the amplifier, $\nu_a=\omega_a/(2\pi)$.

	M (kg)	ν (Hz)	Q	L_b (m)	ν_a (Hz)
Bar	2.3×10^3	896.8	5×10^6	3	—
Transducer	6.1	898.4	2×10^6	—	900

here $\mu\equiv M_{tr}/M_b\ll1$, and M_b, M_{tr}, Q_b, and Q_{tr} are the masses and Q factors of the bar and transducer, respectively. The forces $F_{ba}(\omega)$ and $F(\omega)$ are the back-action force acting both on the bar and transducer and the external force, impinging on the bar. By solving these equations, we obtain the displacements $x(\omega)$, $y(\omega)$ and then their difference $[x(\omega)-y(\omega)]$, fed to the amplifier. Then, the expression for the force signal noise at the SQL is given by

$$S_F^{\mathrm{SQL}}(\omega)=\frac{\hbar}{\mu M_{tr}\omega^4}P(\omega)^{1/2}\|B(\omega)\|, \tag{27}$$

where $P(\omega)\equiv[(1+\mu)\omega^2-\omega_b^2]^2+\omega_b^4/Q_b^2$, ω_b and ω_{tr} are the resonant angular frequencies of the bar and the transducer, correspondingly, and $\|B(\omega)\|$ is the determinant of the matrix $\mathcal{B}(\omega)$. In Table I we report the design parameters of the AURIGA detector in the present configuration [15].

Figure 8 shows the square root of $S_{hh}(\omega)$ in the case of the SQL (solid line) and in the case of optimization at a particular amplifier frequency ν_a (dashed line). The dashed line has only one minimum, whereas the solid one has two more minima. This is due to the optimization process. In fact, to optimize at a particular amplifier frequency means to differentiate the total spectral density with respect to the displacement noise spectral density, which entails the suppression of the poles of the noise transfer functions.

The solid line in Fig. 8 is obtained by using Eq. (27) as the total spectral density in Eq. (6), with $M_{eff}=M_b/2$ and

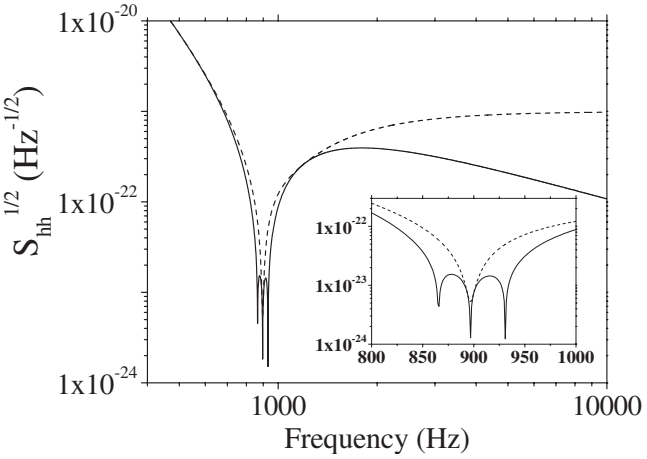

FIG. 8. $S_{hh}^{1/2}$ in the SQL case (solid line) and in the optimized case $\nu_a=900$ Hz (dashed line). The inset represents a zoom of $S_{hh}^{1/2}$ around 900 Hz. AURIGA parameters as in Table I.

$L_{eff}=4L_b/\pi^2$ [17], while the external force noise power spectral density for the dashed line is given by

$$S_F(\omega)=\frac{\hbar}{2\mu M_{tr}\omega^4}P(\omega_a)^{1/2}\|B(\omega_a)\|\left[\frac{\|B(\omega)\|^2}{\|B(\omega_a)\|^2}+\frac{P(\omega)}{P(\omega_a)}\right]. \tag{28}$$

The external force transfer function is expressed by

$$H_F(\omega)=\frac{-M_{tr}\omega^2}{\|B(\omega)\|}, \tag{29}$$

while the back-action transfer function is given by

$$H_{F_{ba}}(\omega)=\frac{M_b}{\|B(\omega)\|}\left[\omega_b^2\left(1+\frac{i}{Q_b}\right)-\omega^2-\mu\omega^2\right]. \tag{30}$$

As expected by an impedance matching, the overall sensitivity of two coupled oscillators and a single oscillator remains the same. In fact, by assuming $\omega_b=\omega_{tr}=\omega_o$, $Q_b=Q_{tr}=Q$, and $M_b=m_o$, one can demonstrate that Eq. (27) reduces to Eq. (18), with the minimum scaled from $\hbar m_o\omega_o^2/Q$ to $(\hbar m_o\omega_o^2/Q)\mu$ over the narrower frequency range $\omega_o(1\pm\sqrt{\mu})$.

D. Thermal noise contribution

Another physical limit exists on the minimum momentum of a test mass, a phenomenon usually referred to as *thermal noise* that constitutes a generalization of Brownian motion [22]. The fluctuation-dissipation theorem, enunciated by Callen and Welton [29], establishes a relationship between the thermal fluctuations and the dissipations of a linear system. In order to calculate the total noise budget of a GW detector, the thermal noise spectrum can be estimated by measuring losses of mechanical oscillators.

The sensitivity of GW detectors could also be limited by thermal noise, and therefore it is important to study its contributions [22,30]. In fact, by considering the thermal noise in the case of a bar coupled with a resonant transducer, we lose two orders of magnitude in the $S_{hh}^{1/2}(\omega)$ spectrum, with temperature $T=4.5$ K and $Q\sim10^6$.

Let us consider an external force, for example the GW force, acting on the bar and the back-action force acting both on bar and transducer. When we add the thermal noise to the input force noise power spectral density, $S_F(\omega)$, we obtain the following total spectral density:

$$S_{\mathrm{tot},F}(\omega)=S_F(\omega)+\frac{G_x(\omega)}{|H_F(\omega)|^2}. \tag{31}$$

The term $G_x(\omega)/|H_F(\omega)|^2$ is the input force thermal noise power spectral density;

$$G_x(\omega)=\frac{-4k_BT}{\omega}\mathrm{Im}[H_{F_{ba}}(\omega)] \tag{32}$$

is the output displacement thermal noise power spectral density [29]; k_B is Boltzmann's constant; and $H_F(\omega)$ and $H_{F_{ba}}(\omega)$ are given by Eqs. (29) and (30), respectively.

It is important to stress that we continue to use the term "SQL curves" even if it is improper in the presence of ther-

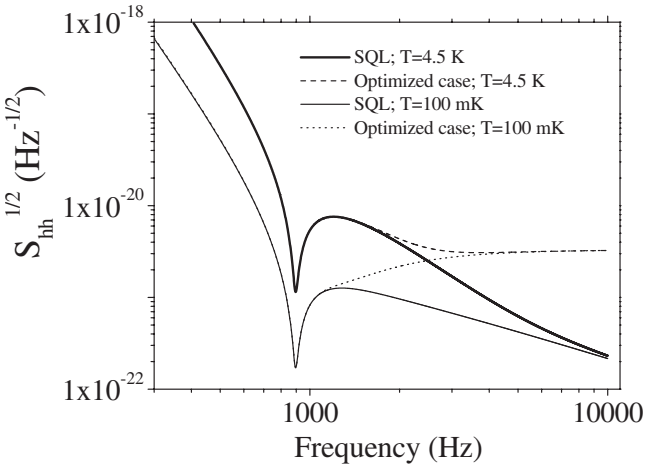

FIG. 9. Square root of S_{hh} in the SQL case and in the optimization case for two different antenna temperatures T. AURIGA parameters as in Table I.

mal noise, meaning that we optimize at any amplifier frequency. Of course, SQL sensitivity can only be achieved if thermal noise is below the back-action noise level.

The SQL curves in Fig. 9 have been calculated by

$$[S_{hh}^{\mathrm{SQL}}(\omega)]^{1/2} = \frac{2[S_{tot,F}^{\mathrm{SQL}}(\omega)]^{1/2}}{M_{eff}L_{eff}\omega^2}, \tag{33}$$

where $S_{\mathrm{tot},F}^{\mathrm{SQL}}(\omega) = S_F^{\mathrm{SQL}}(\omega) + G_x(\omega)/|H_F(\omega)|^2$ and the bold solid and thin lines correspond to temperatures $T=4.5$ K and $T=100$ mK, respectively.

The dashed curve, obtained for $T=4.5$ K, and the dotted curve for $T=100$ mK, in Fig. 9, correspond to

$$S_{hh}^{1/2}(\omega) = \frac{2S_{\mathrm{tot},F}^{1/2}(\omega)}{M_{eff}L_{eff}\omega^2}, \tag{34}$$

with $S_{\mathrm{tot},F}(\omega)$ given by Eq. (31) and $S_F(\omega)$ obtained by optimizing the amplifier at a frequency $\nu_a=900$ Hz.

To be more specific, the bold solid and dashed lines shown in Fig. 9 correspond to the solid and dashed lines in Fig. 8 with the addition of the thermal noise contribution. It is worth pointing out the differences in the sensitivity: it ranges from $\sim 10^{-23}$ $\mathrm{Hz}^{-1/2}$ (see Fig. 8) to $\sim 10^{-21}$ $\mathrm{Hz}^{-1/2}$ for a temperature of 4.5 K and to $\sim 10^{-22}$ $\mathrm{Hz}^{-1/2}$ for 100 mK (see Fig. 9) in correspondence of the bar resonant frequency. Notice that, as we anticipated, the sensitivity loses two magnitude orders at $T=4.5$ K.

In Fig. 9, where the minimum of $S_{hh}^{1/2}$ is ~ 900 Hz, we are not able to discriminate between the resonance frequencies of the bar and transducer. This occurs because the same resonant frequencies are present in $G_x(\omega)$ and $|H_F(\omega)|^2$, and in their ratio they cancel out.

Of course, the curves in Fig. 8, obtained without the thermal noise contribution, are better at the frequency where we have optimized the amplifier than the curves in Fig. 9 (obtained with the addition of thermal noise). In order to reach the SQL, the thermal noise must be reduced by a suitable choice of material Q factor and temperature T.

IV. CONCLUSIONS

We have investigated the sensitivity of coupled harmonic oscillators to interactions with a weak classical force. Starting from a single particle and harmonic oscillator, we estimated the force sensitivity of two harmonic oscillators, resonating at different or equal frequencies. We applied the SQL formalism to two GW detectors, DUAL and AURIGA, as concrete examples of weak classical forces measured by displacement probes at the SQL.

The SQL sensitivity obtained by considering an interacting test mass is better than the free mass SQL, which demonstrates the advantage of a quantum mechanical harmonic oscillator. Moreover, even if we do not operate the probe at the SQL, and optimize the amplifier at $\nu_a=1$ kHz, we find in a small interval around the oscillator resonant frequency an amplitude force $F_{\mathrm{min}}^{o} \simeq 2.1\times 10^{-14}$ N ($Q=10$ and $\tau_F=1$ s), slightly lower than the one obtained for a free particle of the same mass (1 kg), $F_{\mathrm{min}}^{fm} \simeq 6.5\times 10^{-14}$ N ($\tau_F=1$ s).

We studied two coupled harmonic oscillators, with equal masses and different resonance frequencies (as a model for the DUAL detector), using typical design parameters of the DUAL detector. We found the very low SQL force noise, $S_D^{1/2} \simeq 3\times 10^{-15}$ $\mathrm{N/Hz}^{1/2}$, at the two oscillators' resonant frequencies. Moreover, the value of the displacement power spectral density $S_x=10^{-45}$ m^2/Hz produces an extremely flat force noise curve, i.e., $S_D^{1/2} \simeq 10^{-12}$ $\mathrm{N/Hz}^{1/2}$ in a frequency band larger than 700 Hz: for instance, a DUAL detector of $M_{eff}=10^3$ kg and $L_{eff}=1$ m will reach a strain sensitivity of $\sim 2.3\times 10^{-23}$ $\mathrm{Hz}^{-1/2}$ at 1.5 kHz.

The lowest achieved experimental displacement noise is $S_x \simeq 2.5\times 10^{-39}$ m^2/Hz [31] in the kHz range, as two different kinds of implemented readout have already demonstrated in bench experiments, i.e., the optomechanical and capacitive schemes, based on Fabry-Perot cavities [25,32] and SQUID amplifiers [33], respectively. Both readouts could reach, in the near future, displacement sensitivities $S_x \simeq 10^{-44}$ m^2/Hz. However, to achieve the 10^{-45} m^2/Hz sensitivity, which allows one to optimize the noise curve for a DUAL detector (Fig. 7), nonresonant mechanical amplifiers or selective readout may be used [14,27].

Finally, we applied the concept of two strongly coupled harmonic oscillators, with different masses and the same resonance frequencies, to the AURIGA detector. By focusing our attention on the SQL power spectral density $S_{hh}^{1/2}$, we found a value of roughly 10^{-24} $\mathrm{Hz}^{-1/2}$ at the bar resonant frequency by neglecting the thermal noise contribution, and we obtained $S_{hh}^{1/2} \simeq 10^{-21}$ $\mathrm{Hz}^{-1/2}$ and 10^{-22} $\mathrm{Hz}^{-1/2}$ for a temperature of 4.5 K and 100 mK, respectively.

ACKNOWLEDGMENTS

We are grateful to Giovanni A. Prodi and Michele Bonaldi for stimulating and helpful discussions. We also thank William Joseph Weber for a careful reading of the manuscript.

[1] V. B. Braginsky and F. Ya. Khalili, *Quantum Measurement* (Cambridge University Press, Cambridge, England, 1992).
[2] W. A. Edelstein, J. Hough, J. R. Pugh, and W. Martin, J. Phys. E **11**, 710 (1978).
[3] C. M. Caves, K. S. Thorne, R. W. P. Drever, V. D. Sandberg, and M. Zimmermann, Rev. Mod. Phys. **52**, 341 (1980).
[4] T. Briant, O. Arcizet, T. Caniard, P.-F. Cohadon, A. Heidmann, and M. Pinard, J. Phys.: Conf. Ser. **32**, 288 (2006).
[5] H. M. Wiseman, Phys. Rev. A **51**, 2459 (1995).
[6] G. M. D'Ariano, M. F. Sacchi, and R. Seno, Nuovo Cimento Soc. Ital. Fis., B **114**, 775 (1999).
[7] K. Bencheikh, J. A. Levenson, P. Grangier, and O. Lopez, Phys. Rev. Lett. **75**, 3422 (1995).
[8] N. Imoto, H. A. Haus, and Y. Yamamoto, Phys. Rev. A **32**, 2287 (1985).
[9] P. Grangier, J. A. Levenson, and J.-P. Poizat, Nature (London) **396**, 537 (1998).
[10] V. B. Braginsky and F. Ya. Khalili, Phys. Lett. A **147**, 251 (1990).
[11] R. G. Knobel and A. N. Cleland, Nature (London) **424**, 291 (2003).
[12] M. D. LaHaye, O. Buu, B. Camarota, and K. C. Schwab, Science **304**, 74 (2004).
[13] A. Buonanno and Y. Chen, Phys. Rev. D **64**, 042006 (2001).
[14] M. Bonaldi, M. Cerdonio, L. Conti, M. Pinard, G. A. Prodi, L. Taffarello, and J. P. Zendri, Phys. Rev. D **68**, 102004 (2003).
[15] L. Baggio *et al.*, Phys. Rev. Lett. **95**, 081103 (2005).
[16] V. B. Braginsky, M. L. Gorodetsky, F. Ya. Khalili, and K. S. Thorne, Phys. Rev. D **61**, 044002 (2000).
[17] C. W. Misner, K. S. Thorne, and J. A. Wheeler, *Gravitation* (W. H. Freeman, San Francisco, 1973).
[18] R. Mezzena, A. Vinante, P. Falferi, S. Vitale, M. Bonaldi, G. A. Prodi, M. Cerdonio, and M. B. Simmonds, Rev. Sci. Instrum. **72**, 3694 (2001).
[19] P. Falferi, M. Bonaldi, M. Cerdonio, A. Vinante, R. Mezzena, G. A. Prodi, and S. Vitale, Appl. Phys. Lett. **88**, 062505 (2006).
[20] S. Vitale, M. Cerdonio, E. Coccia, and A. Ortolan, Phys. Rev. D **55**, 1741 (1997).
[21] J. C. Price, Phys. Rev. D **36**, 3555 (1987).
[22] P. Saulson, *Fundamentals of Interferometric Gravitational Wave Detectors* (World Scientific, Singapore, 1994).
[23] V. Fafone, Class. Quantum Grav. **23**, S223 (2006).
[24] A. E. H. Love, *A Treatise on the Mathematical Theory of Elasticity* (Dover, New York, 1944).
[25] T. Briant, M. Cerdonio, L. Conti, A. Heidmann, A. Lobo, and M. Pinard, Phys. Rev. D **67**, 102005 (2003).
[26] P. Rapagnani, Nuovo Cimento Soc. Ital. Fis., C **5**, 385 (1982).
[27] J. H. Paik, G. M. Harry, and T. Stevenson, in *Proceedings of the Seventh Marcel Grossmann Meeting on General Relativity, Stanford, 1994*, edited by R. T. Jantzen, G. Mac Kreiser, and R. Ruffini (World Scientific, Singapore, 1996), p. 1483.
[28] A. Vinante, R. Mezzena, G. A. Prodi, S. Vitale, M. Cerdonio, M. Bonaldi, and P. Falferi, Rev. Sci. Instrum. **76**, 074501 (2005).
[29] H. B. Callen and T. A. Welton, Phys. Rev. **83**, 34 (1951).
[30] K. Yamamoto, Ph.D. thesis, Graduate School of Science, University of Tokyo, 2000 (unpublished).
[31] L. Conti, M. De Rosa, and F. Marin, J. Opt. Soc. Am. B **20**, 462 (2003).
[32] J.-P. Richard, Phys. Rev. D **46**, 2309 (1992).
[33] M. Bonaldi, M. Cerdonio, L. Conti, G. A. Prodi, L. Taffarello, and J. P. Zendri, Class. Quantum Grav. **21**, S1155 (2004).
[34] S. L. Danilishin, J. Phys.: Conf. Ser. **66**, 012059 (2007).
[35] Here, the term "fundamental" refers to the continuous measurement of the position of a test mass. On the contrary, an external classical force acting on a quantum system can be observed with arbitrary precision by a properly designed probe; in fact, the operator algebra associated to a classical force is commutative and so no fundamental restriction on the precision of classical force measurements exists (see, e.g., Ref. [34]).